ISSN 1674-1056
http://cpb.iphy.ac.cn
http://iopscience.iop.org/cpb
中国物理 B
Chinese Physics
中国物理 Chinese Physics B

Temperature dependence on the electrical and physical performance of InAs/AlSb heterojunction and high electron mobility transistors

Jing Zhang(张静), Hongliang Lv(吕红亮), Haiqiao Ni(倪海桥), Zhichuan Niu(牛智川), Yuming Zhang(张玉明)

Citation: Chin. Phys. B . 2018, 27(9): 097201. **doi:** 10.1088/1674-1056/27/9/097201

Journal homepage: http://cpb.iphy.ac.cn; http://iopscience.iop.org/cpb

What follows is a list of articles you may be interested in

Room-temperature operating extended short wavelength infrared photodetector based on interband transition of InAsSb/GaSb quantum well

Ling Sun(孙令), Lu Wang(王禄), Jin-Lei Lu(鲁金蕾), Jie Liu(刘洁), Jun Fang(方俊), Li-Li Xie(谢莉莉), Zhi-Biao Hao(郝智彪), Hai-Qiang Jia(贾海强), Wen-Xin Wang(王文新), Hong Chen(陈弘)

Chin. Phys. B . 2018, 27(4): 047209. **doi:** 10.1088/1674-1056/27/4/047209

Effect of Nb doping on microstructures and thermoelectric properties of $SrTiO_3$ ceramics

Da-Quan Liu(刘达权), Yu-Wei Zhang(张玉伟), Hui-Jun Kang(康慧君), Jin-Ling Li(李金玲), Xiong Yang(杨雄), Tong-Min Wang(王同敏)

Chin. Phys. B . 2018, 27(4): 047205. **doi:** 10.1088/1674-1056/27/4/047205

Uncertainties of clock and shift operators for an electron in one-dimensional nonuniform lattice systems

Long-Yan Gong(巩龙延), You-Gen Ding(丁友根), Yong-Qiang Deng(邓永强)

Chin. Phys. B . 2017, 26(11): 117201. **doi:** 10.1088/1674-1056/26/11/117201

Plasma-assisted surface treatment for low-temperature annealed ohmic contact on AlGaN/GaN heterostructure field-effect transistors

Lei Wang(王磊), Jiaqi Zhang(张家琦), Liuan Li(李柳暗), Yutaro Maeda(前田裕太郎), Jin-Ping Ao(敖金平)

Chin. Phys. B . 2017, 26(3): 037201. **doi:** 10.1088/1674-1056/26/3/037201

High temperature characteristics of bilayer epitaxial graphene field-effect transistors on SiC Substrate

Ze-Zhao He(何泽召), Ke-Wu Yang(杨克武), Cui Yu(蔚翠), Qing-Bin Liu(刘庆彬), Jing-Jing Wang(王晶晶), Jia Li(李佳), Wei-Li Lu(芦伟立), Zhi-Hong Feng(冯志红), Shu-Jun Cai(蔡树军)

Chin. Phys. B . 2016, 25(6): 067206. **doi:** 10.1088/1674-1056/25/6/067206

Temperature dependence on the electrical and physical performance of InAs/AlSb heterojunction and high electron mobility transistors*

Jing Zhang(张静)[1,2], Hongliang Lv(吕红亮)[1,†], Haiqiao Ni(倪海桥)[2], Zhichuan Niu(牛智川)[2], and Yuming Zhang(张玉明)[1]

[1] School of Microelectronics, Xidian University and Key Laboratory of Wide Band-Gap Semiconductor Materials and Devices, Xi'an 710071, China
[2] State Key Laboratory for Superlattices and Microstructures, Institute of Semiconductors, Chinese Academy of Sciences, Beijing 100083, China

(Received 5 March 2018; revised manuscript received 12 June 2018; published online 10 August 2018)

In this report, the effect of temperature on the InAs/AlSb heterojunction and high-electron-mobility transistors (HEMTs) with a gate length of 2 μm are discussed comprehensively. The results indicate that device performance is greatly improved at cryogenic temperatures. It is also observed that the device performance at 90 K is significantly improved with 27% lower gate leakage current, 12% higher maximum drain current, and 22.5% higher peak transconductance compared to 300 K. The temperature dependence of mobility and the two-dimensional electron gas concentration in the InAs/AlSb heterojunction for the temperature range 90 K–300 K is also investigated. The electron mobility at 90 K (42560 $cm^2/V{\cdot}s$) is 2.5 times higher than its value at 300 K (16911 $cm^2/V{\cdot}s$) because of the weaker lattice vibration and the impurity ionization at cryogenic temperatures, which corresponds to a reduced scattering rate and higher mobility. We also noted that the two-dimensional electron gas concentration decreases slightly from 1.99×10^{12} cm^{-2} at 300 K to 1.7×10^{12} cm^{-2} at 90 K with a decrease in temperature due to the lower ionization at cryogenic temperature and the nearly constant ΔE_c.

Keywords: temperature, mobility, two-dimensional electron gas, InAs/AlSb HEMT

PACS: 72.10.–d, 73.40.Kp, 81.05.Ea **DOI:** 10.1088/1674-1056/27/9/097201

1. Introduction

In recent years, InAs/AlSb HEMTs have become one of the most promising candidates for high-speed, low-power, and low-noise applications.[1,2] A very important application of these transistors is for low noise amplifiers (LNA) that are used in deep space exploration, and are operated primarily at cryogenic temperatures to improve the sensitivity of detection.

During the past twenty years, InP HEMTs have been the dominant force in microwave millimeter wave applications.[3,4] Compared with InP HEMTs, InAs has a higher electron mobility and saturation drift speed. Moreover, InAs/AlSb HEMTs exhibit a two-dimensional electron gas (2-DEG) distribution in the channel due to the small lattice mismatch between the InAs and AlSb and the large conduction band offset (about 1.35 eV) that can form deep quantum wells. Therefore, the application of InP HEMTs for use in cryogenic LNAs has recently been challenged by InAs/AlSb HEMTs. In Ref. [5], the first demonstration of an InAs/AlSb HEMT LNA at cryogenic temperatures was reported. At room temperature, the three-stage amplifier exhibited a transducer gain of 29 dB and a noise temperature of 150 K with 17.6 mW power consumption. At cryogenic temperatures, the optimum drain voltage for best noise performance was reduced from 0.55 V to 0.3 V, demonstrating the very low-power and low-voltage capabilities of InAs/AlSb HEMTs-based low-noise amplifiers. InAs/AlSb HEMTs are typical 2DEG-based devices with electrical characteristics that are very sensitive to the operating temperature. The cryogenic characteristics of InAs/AlSb HEMTs are determined by the temperature dependency of the electron mobility and 2-DEG in the InAs channel. The characterization of electron mobility and 2-DEG at different temperatures will assist in improving the general understanding of the change mechanism of the drain current, gate-leakage currents and transconductance.

In this work, the temperature effect on InAs/AlSb heterojunction and HEMTs are comprehensively discussed. The results indicate that device performance is greatly improved at low temperatures. It has also been observed that the leakage current decreases with a reduction of the to 90 K because of the Schottky leakage current component and the hole leakage current component caused by the impact ionization effect decreased. The decrease of the gate–leakage currents with temperature is a clear advantage for devices operating at cryogenic temperatures. The temperature dependence of the mobility and the two-dimensional electron gas concentration in InAs/AlSb heterojunctions in the temperature range 90 K–300 K is also investigated. The lower lattice vibration and the impurity ionization at cryogenic temperatures correspond to a reduced scattering rate and higher mobility. The two-dimensional electron gas concentration decreases slightly with the decrease of temperature due to the lower ionization at cryogenic and the nearly constant ΔE_c.

*Project supported by the Advanced Research Foundation of China (Grant No. 914xxx803-051xxx111), the National Defense Advanced Research Project of China (Grant No. 315xxxxx301), and the National Defense Innovation Program of China (Grant No. 48xx4).

†Corresponding author. E-mail: hllv@mail.xidian.edu.cn

© 2018 Chinese Physical Society and IOP Publishing Ltd

2. Epitaxial structure and device fabrication

Before device fabrication, the material is grown by molecular beam epitaxy (MBE). The material structure and its energy band diagram are illustrated in Figs. 1(a) and 1(b). The epitaxial materials are grown on 2-in semi-insulating GaAs substrates. A composite AlSb/$Al_{0.7}Ga_{0.3}Sb$ metamorphic buffer layer with a thickness of 1.45 μm is utilized to relax the 8% compressive lattice mismatch between the GaAs substrate and the active layers of the device. The HEMT active layers above the metamorphic buffer layers consist of a 50 nm AlSb HEMT buffer layer, a 15 nm InAs channel, a 5 nm AlSb spacer, a 2×10^{12} cm^{-2} Si δ-doped plane inserted in four monolayers of InAs (∼1.2 nm), and an 8 nm AlSb Schottky layer. On the top, there is a 4 nm $In_{0.5}Al_{0.5}As$ protection layer and a 5 nm InAs contact layer. A root-mean-square roughness of 1.27 nm is measured on the as-grown surface by AFM is shown in Fig. 2.

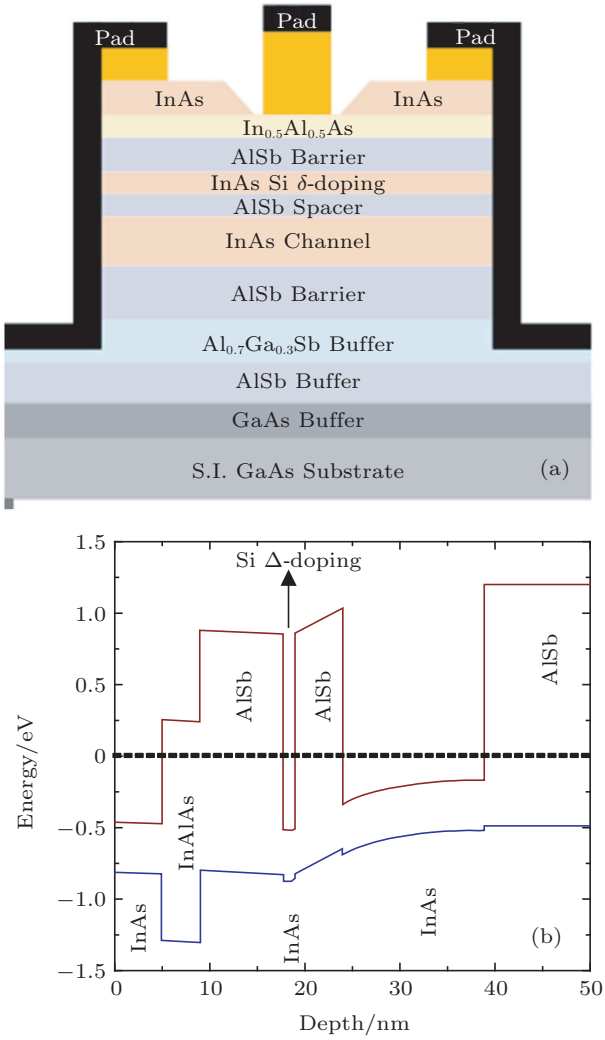


Fig. 1. (color online) (a) Schematic InAs/AlSb HEMT and (b) the energy band diagram.

An alloyed Ohmic contact is formed by e-beam evaporation of Pd/Ti/Pt/Au (20/30/30/30 nm), following by RTA at 300 °C for 20 s. The contact resistance R_c and contact resistivity ρ_c are 0.116 Ω·mm and 3.50×10^{-7} Ω·cm^2, respectively, for TLM at 300 K. Optical images of TLM pattern, *I*–*V* curves of two contacts with different d_n, and R_{tot} as a function of d_n are shown in Figs. 3(a)–3(c), respectively.

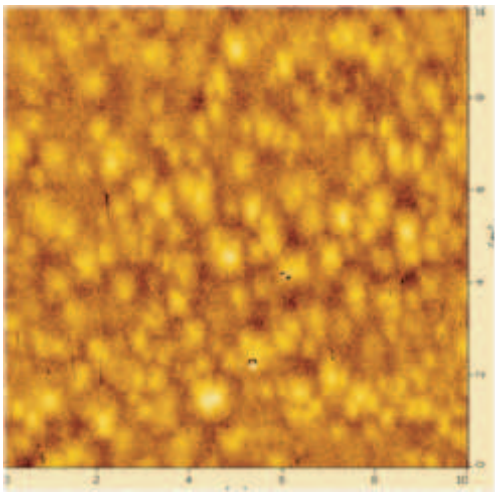


Fig. 2. (color online) AFM of InAs cap surface.

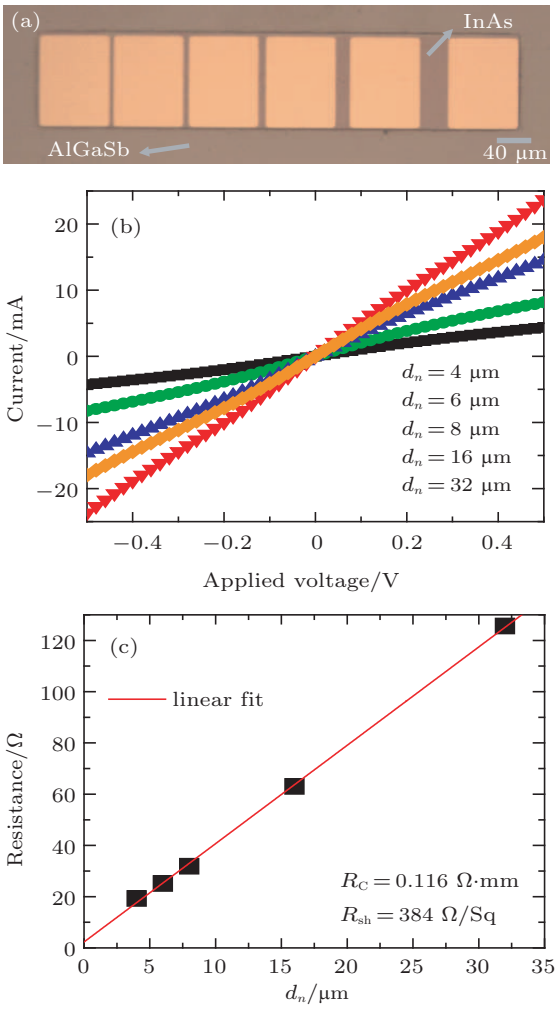


Fig. 3. (color online) (a) Optical image of TLM pattern, (b) *I*–*V* curves of two contacts with different d_n at 300 K, and (c) R_{tot} as a function of d_n.

Before Schottky gate metal deposition, gate recess etching is performed using a citric acid/H_2O_2 solution in order to avoid gate-to-source and gate-to-drain conduction, because of the highly doped InAs cap layer. Then, the Schottky gate metal is deposited by e-beam evaporation of Ti/Pt/Au (20/20/300 nm). Finally, a probing pad is deposited by e-beam evaporation of Ti/Au (20/300 nm). A gate width of 50 μm and a gate length of 2 μm are used, as shown in Fig. 4.

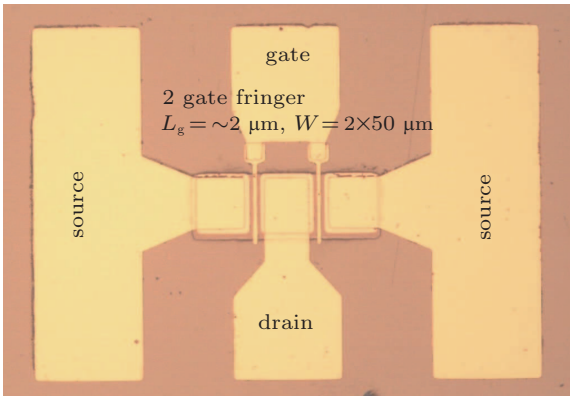


Fig. 4. (color online) Optical image of InAs/AlSb HEMT.

3. Results and discussion

3.1. The cryogenic characteristics of InAs/AlSb heterojunction

The cryogenic characteristics of InAs/AlSb heterojunctions are determined by the cryogenic characteristics of a 2-DEG in an InAs channel, in which the temperature dependency of mobility and the density of electrons is important.

The electron mobility μ refers to the average speed of electrons units under the influence of the electric field, which is determined by scattering mechanism. The value of μ can be obtained from the relaxation time τ, which is inversely proportional to the scattering probability P;

$$\mu = q\langle\tau\rangle/m^*, \tag{1}$$

where m^* is the effective mass of the electron.

There are three primary scatter mechanisms for mobility in the InAs channel: ionized impurity scattering, lattice vibration scattering, and interface roughness scattering.[6–8]

$$\frac{1}{\mu} = \sum_i \frac{1}{\mu_i}. \tag{2}$$

As the temperature decreases, the lattice vibration and the impurity ionization decrease, which results in reduced scattering rate and higher mobility. The interface roughness scattering is associated with the two-electron gas density.

Figure 5 shows Hall measurement results in the temperature range from 90 K to 300 K after the completion of material growth. It can be seen that the electron mobility increases significantly with a decrease in temperature. The electron mobility at 90 K (42560 $cm^2/V{\cdot}s$) is 2.5 times higher than its value at 300 K (16911 $cm^2/V{\cdot}s$).

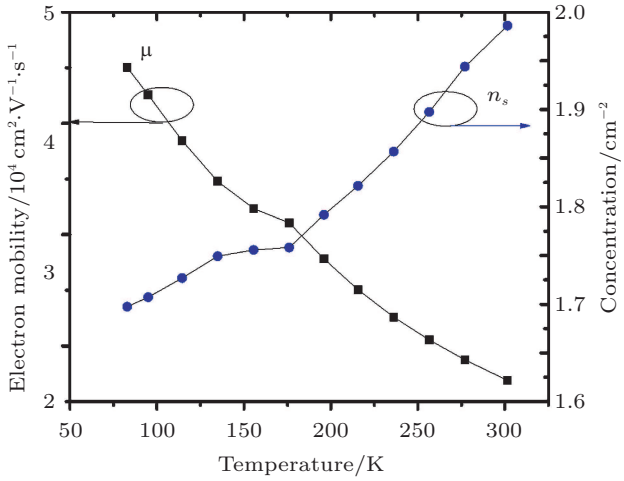


Fig. 5. (color online) The electron mobility μ and n_s versus temperature.

The 2-DEG is generated in the InAs channel on the side of the InAs/AlSb heterostructure It can be seen from Fig. 5 that the two-dimensional electron gas concentration n_s decreases from 1.99×10^{12} cm^{-2} at 300 K to 1.71×10^{12} cm^{-2} at 90 K with a decrease in temperature. This can be explained as follows.

(i) From 300 K to 175 K, the concentration n_s decreased rapidly because the ionization rate of impurities decreased significantly. Below 175 K, the concentration decreased slowly because the ionization rate of impurities cannot be significantly reduced any further.

(ii) The relationship between the InAs bandgap and temperature can be expressed by

$$E_g = 0.42 - 2.5\times10^{-4}T^2/(T+75). \tag{3}$$

The relationship between the AlSb gap width and temperature can be expressed by

$$E_g = 1.687 - 4.97\times10^{-4}T^2/(T+213). \tag{4}$$

The conduction band offset ΔE_c[9] at different temperatures are shown in Table 1. It can be seen that ΔE_c is almost unchanged with a decrease in temperature. Therefore, the corresponding two-dimensional electron gas concentration does not change significantly with temperature because the limiting effect on electrons is almost constant.

Table 1. ΔE_c at different temperatures.

T	300 K	200 K	100 K
E_g(InAs)/eV	0.36	0.38	0.41
E_g(AlSb)/eV	1.61	1.64	1.67
ΔE_c	1.25	1.26	1.26

It can be seen from the previous analysis that the 2-DEG concentration decreases slightly with a decrease in temperature because of the diminished ionization at cryogenic temperatures.

3.2. The cryogenic characteristics of InAs/AlSb HEMT

Electrical measurements are performed using a cryogenic probe station Lakeshore CRX-4K to connect an Agilent B1500A at room temperature (300 K) and at a cryogenic temperature (90 K). When the temperature is reduced to 90 K, the device performance is greatly improved.

Figure 6 shows that the gate leakage current is significantly reduced as the temperature decreases to 90 K and increases with the drain voltage up to 0.5 V. At room temperature, the measured gate leakage current is −59.9 mA/mm, while at 90 K the device has a 27% lower gate leakage current (−47.24 mA/mm). Here, the total leakage current I_g can be expressed by[10,11]

$$I_g = I_{ge} + I_{gh}, \tag{5}$$

where I_{ge} is the Schottky leakage current and I_{gh} is the hole current component generated due to the impact ionization effect.

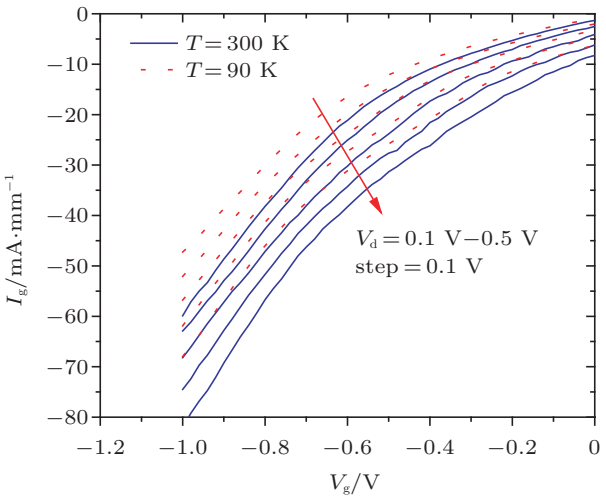


Fig. 6. (color online) I_g (V_g) with V_d ranging from 0.1 V to 0.5 V in steps of 0.1 V at 300 K (solid lines) and 90 K (dot lines).

i) The Schottky leakage current as a function of temperature is given by

$$I_{ge} = SAT^2 \exp\left(\frac{-e\phi_{Bn}}{kT}\right), \tag{6}$$

where S is the area of the gate electrode, T is the thermodynamic temperature, e is electron charge, k is Boltzmann's constant, and ϕ_{Bn} is the Schottky barrier height. Here the Effective Richardson constant

$$A* = \frac{4\pi e m_n^* k^2}{h^3}.$$

Thus

$$I_{ge} \infty T^2 \exp\left(\frac{1}{T}\right).$$

It can be seen that I_{ge} decreases with a decrease in temperature.

ii) The impact ionization effect means that the collision between carriers and lattice atoms will generate redundant electron–hole pairs because the carriers in the channel experience an increase in energy as the applied voltage is increased. Thus, it can be seen from Fig. 6 that I_g increases with the drain voltage up to 0.5 V. However, the energy of the carrier decreases with a decrease in temperature, thus I_{gh} caused by the impact ionization effect is reduced.

Figure 7 shows the output characteristic curve I_d–V_d of InAs/AlSb HEMTs measured at 90 K and 300 K for different gate voltages from −1 V to 0 V.

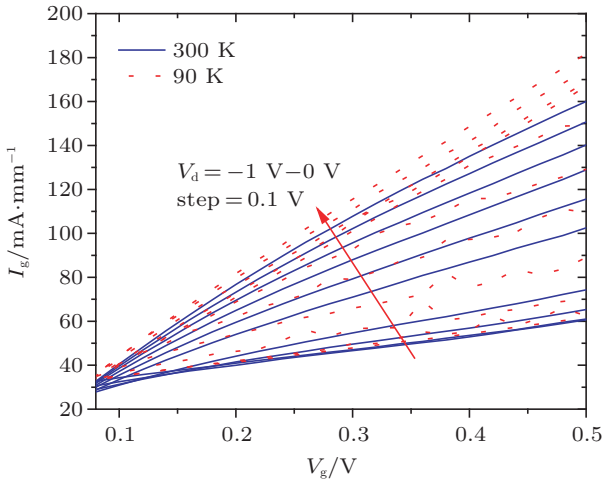


Fig. 7. (color online) I_d (V_d) with V_g ranging from −1 V to 0 V in steps of 0.1 V at 300 K (solid lines) and 90 K (dot lines).

In the linear region, the drain current is given by

$$I_d = \frac{1}{2}\mu C \frac{W}{L}[2(V_g - V_p)V_d - V_d^2]. \tag{7}$$

In the saturation region, the drain current is given by

$$I_d = \frac{1}{2}\mu C \frac{W}{L}(V_g - V_p)^2, \tag{8}$$

where C is the equivalent capacitance per unit area, V_p is the pinch-off voltage, W is the device width, and L is the channel length. Thus $I_d \propto \mu$.

It can be seen from Fig. 7 that the drain current increases with a decrease in the temperature because $I_d \propto \mu$. At a V_g of 0 V, the maximum drain current of the fabricated devices is 160 mA/mm at room temperature. At 90 K, I_d increases up to 181.8 mA/mm. Therefore, the required drain voltage at a cryogenic temperature is lower than that at room temperature for the same output current, and the corresponding power consumption will decrease. As shown in Fig. 7, a large leakage current is present in our device. This result is unexpected. It can be explained by considering that, sidewall etching subsequent to the mesa etching used in our fabrication process

is performed using citric acid/H_2O_2 solution to avoid gate-to-channel conduction at the mesa edge. The large leakage current is therefore due to insufficient sidewall etching. In addition, it should be noted that gate-to-channel conduction may also result in a large leakage current due to the absence of passivation after mesa etching. This could be another possible explanation for the large leakage current in our device. Since leakage is included in the I_d of the device, this parameter is also increased with a decrease in temperature because the electron mobility μ of the InAs material will be greatly improved at cryogenic temperatures.

Figure 8(a) shows the relationship between transconductance and the gate voltage for the drain voltages of 0.1 to 0.5 V at two different temperatures. It can be seen from Fig. 8(a) that the transconductance peak requires a V_g of approximately −0.62 V at 90 K and −0.46 V at 300 K.

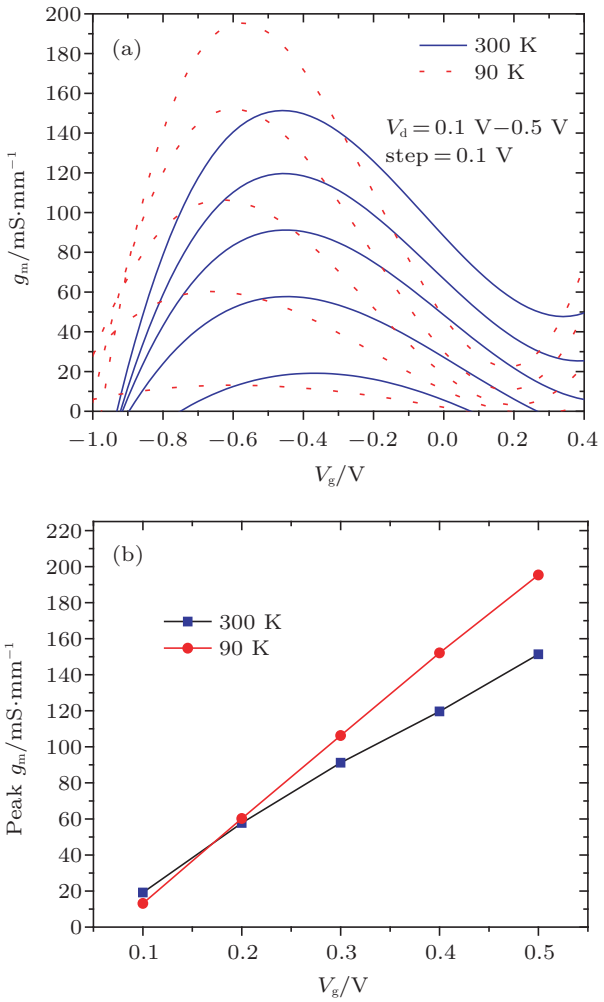


Fig. 8. (color online) (a) g_m (V_g) at 300 K and 90 K for drain voltages of 0.1 to 0.5 V. (b) Peak g_m (V_d) at 300 K and 90 K.

The relationship between the transconductance and the drain voltages can be expressed by

$$g_m = \frac{\partial I_d}{\partial I_g}. \tag{9}$$

At low drain voltages, the contribution of the 2-DEG is greater than the electron mobility, so a larger transconductance value is measured at room temperature. Figure 8(b) shows the relationship between the transconductance peaks and the drain voltage at two different temperatures. It can be seen from Fig. 8(b) that the transconductance peaks are 13.12 mS/mm at 90 K and 19.15 mS/mm at 300 K for $V_d = 0.1$ V. At 0.2 V, the two transconductance peaks are approximately 60 mS/mm. However, compared with wider bandgap semiconductors, the 2-DEG concentration of narrow bandgap semiconductors decreases slightly with a decrease in temperature, which causes the degradation of the transconductance at low temperatures, although a low drain voltage is not usually a concern since a minimum threshold value is maintained. This is the advantage of the InAs/AlSb HEMTs at low temperatures. The improvement in the peak g_m at cryogenic temperatures is mainly at a high drain voltage. This is clearly is observed because of the enhanced electron mobility. When V_d is increased to 0.5 V, the increase in the transconductance peak g_m at 90 K is 22.5%. Most applications of InAs/AlSb HEMTs are at less than 0.5 V, and the low-temperature characteristics are more advantageous in this range.

4. Conclusion

We report on studies on the room temperature and cryogenic performance of InAs/AlSb high-electron-mobility transistors (HEMTs) with a gate length of 2 μm, which exhibits significant improvement in device performance at low temperatures. It has been observed that the leakage current decreases when the temperature is reduced to 90 K. This is because of the Schottky leakage current component and the hole leakage current component caused by a decrease of the impact ionization effect. The temperature dependence of the mobility and the two-dimensional electron gas concentration in InAs/AlSb heterojunctions in the temperature range 90 K–300 K is also investigated. The weaken lattice vibration and the impurity ionization at cryogenic temperatures correspond to a reduced scattering rate and higher mobility. The two-dimensional electron gas concentration decreased slightly with a decrease in temperature due to the weakened ionization at cryogenic temperatures and the nearly constant ΔE_c. Overall, it is observed that the performance of InAs/AlSb HEMTs is greatly improved at cryogenic temperatures, which is more amenable to the applications of ultra-high speed and low dissipation circuits.

References

[1] Guan H and Guo H 2017 *Chin. Phys. B* **26** 5 058501
[2] Chiu H C, Lin W Y, Chou C Y, Yang S H, Mai K D, Chiu P C, Hsuehb W J and Chyi J I 2015 *Microelectron. Eng.* **183** 20 17
[3] Liu L, Alt A R, Benedickter H and Bolognesi C R 2012 *IEEE Electron Dev. Lett.* 33

[4] Sun S X, Wei Z C, Xia P H, Wang W B, Duan Z Y, Li Y X, Zhong Y H, Ding P and Jin Z 2018 *Chin. Phys. B* **27** 028502
[5] Moschetti G, Wadefalk N, Nilsson P Å, Abbasi M, Desplanque L, Wallart X and Grahn J 2012 *IEEE Microw. Wirel. Compon. Lett.* **22**
[6] Shojaei B, McFadden A, Shabani J, Schultz B D and Palmstr?m C J 2015 *Appl. Phys. Lett.* **106** 222101
[7] Tschirky T, Mueller S, Lehner Ch A, Falt S, Ihn T, Ensslin K and Wegscheider W 2017 *Phys. Rev. B* **95** 115304
[8] Wang J, Xing J L, Xiang W, Wang G W, Xu Y Q, Ren Z W and Niu Z C 2014 *Appl. Phys. Lett.* **104** 052111
[9] Atsushi N, Herbert K and John H 1989 *Appl. Phys. Lett.* **54** 19
[10] Lin H K, Fan D W, Li Y C, Chiu P C, Chien C Y, Li P W, Chyi J I, Ko C H, Kuan T M, Hsieh M K, Lee W C and Wann C H 2010 *Solid-State Electron.* **54** 505
[11] Lai P H, Fu S I, Hung C W, Tsai Y Y, Chen T P, Chen C W and Liu W C 2006 *Appl. Phys. Lett.* **89** 263503